# RESEARCH ARTICLE



# Biases in sea surface temperature and the annual cycle of Greater Horn of Africa rainfall in CMIP6

# Bradfield Lyon D

Climate Change Institute and School of Earth and Climate Sciences, University of Maine, Orono, Maine, USA

#### Correspondence

Bradfield Lyon, Climate Change Institute and School of Earth and Climate Sciences, 137 Sawyer Hall, University of Maine, Orono, ME 04469, USA.

# Email: bradfield.lyon@maine.edu

**Funding information** 

National Science Foundation, Grant/ Award Number: AGS 1650037

#### **Abstract**

Climatological rainfall across much of the Greater Horn of Africa has a bimodal annual cycle characterized by the short rains from October to December and the long rains from March to May. Previous generations of climate models from the Coupled Model Intercomparison Project (CMIP3 and CMIP5) generally misrepresented the bimodal rainfall distribution in this region by generating too much rainfall during the short rains and too little during the long rains. The peak of the long rains in these models also typically showed a pronounced 1-month lag relative to observations. Here, the ability of 21 CMIP6 models to properly simulate the observed, climatological annual cycle of Greater Horn rainfall is examined, comparing results with CMIP5 and CMIP3. As previous work has shown a connection between Greater Horn climatological rainfall biases and model biases in sea surface temperatures (SSTs), pattern correlations of climatological SST biases are also analysed. For the multi-model mean, it is found that the earlier biases in Greater Horn rainfall and associated SSTs persist in CMIP6. Examining only the three best performing models in each CMIP group reveals the CMIP6 models outperform those in CMIP3, with mixed results regarding improvements over CMIP5. For the best performing CMIP6 models, the SST and 850 hPa wind biases are reduced over the Indian Ocean relative to the other CMIP6 models examined. No statistically significant relationship was identified between CMIP6 model performance and the horizontal resolution of the model. Combined, these results indicate the importance of properly simulating the annual cycle of SSTs in order to successfully model the observed rainfall annual cycle in the Greater Horn.

#### KEYWORDS

Africa, climatology, modelling, precipitation, sea surface temperature

# 1 | INTRODUCTION

The climatological annual cycle of rainfall across the Greater Horn of Africa exhibits considerable spatial variation, however, for much of the region, it is bimodal, featuring the long rains of March–May (MAM; other

seasons denoted similarly) and the short rains of OND. The seasonality of regional rainfall is integral to societal activities, ranging from agricultural practices (Hansen, 2005) to water resources and energy management (Conway *et al.*, 2017) and it shapes environmental conditions necessary for the transmission of vector-borne

Int J Climatol. 2021;1–8. wileyonlinelibrary.com/journal/joc © 2021 Royal Meteorological Society

diseases such as malaria and yellow fever (Thomson et al., 2017; Hamlet et al., 2018). Reliable modelling of the region's climate, including observed linkages to the large-scale climate system, thus has substantial practical implications and scientific value. A well-documented feature of most global climate models participating in both the third and the fifth phases of the Coupled Model Intercomparison Project (CMIP3 and CMIP5, respectively) is their inability to property capture the climatological annual cycle of rainfall in the Greater Horn of Africa. These earlier generations of models tended to generate too little (too much) rainfall during the long rains (short rains) and typically exhibited a 1-month lag in the timing of the peak of the long rains relative to observations (Anyah and Qiu, 2011; Otieno and Anyah, 2013; Yang et al., 2015; Koutroulis et al., 2016; Dunning et al., 2017; Lyon and Vigaud, 2017; Lyon, 2020, among others).

For CMIP5, Lyon (2020) linked the multi-model mean (MMM) biases in the annual cycle of rainfall in the Greater Horn to biases in the monthly climatological sea surface temperatures (SST) in those models. The study found that an atmospheric general circulation model (AGCM) showed good fidelity in reproducing the observed annual cycle in the Greater Horn when the model was forced with observed SSTs (1979-2005). When the AGCM was forced with observed SSTs plus the monthly, MMM CMIP5 SST bias, the atmospheric model's annual cycle in Greater Horn rainfall displayed very similar biases as those seen in the CMIP5 models. The main motivation for this study is to examine whether the biases in the annual cycle of Greater Horn rainfall seen in earlier generations of CMIP models are identified in the latest generation of coupled climate models in CMIP6. Given the importance of CMIP5 SST bias patterns to biases in Greater Horn rainfall, CMIP6 SST bias patterns are also compared to those identified in CMIP5. Model performance as a function of model horizontal spatial resolution is also evaluated across all models within each CMIP group. In addition to examining MMM results, the comparative behaviour of the top three performing models within each CMIP group is considered to test for incremental improvements in the CMIP6 model capability to properly capture the observed annual cycle of Greater Horn rainfall relative to CMIP5 and CMIP3.

### 2 | DATA AND METHODOLOGY

# 2.1 | Coupled model data

Monthly average rainfall, surface temperature (considered SST for ocean areas) and the horizontal components

of the 850 hPa wind were obtained from historical runs of coupled ocean/atmosphere/land surface global climate models, including 21 CMIP6 models (Eyring et al., 2016), with rainfall and surface temperature also obtained for 31 CMIP5 models (Taylor et al., 2012) and 20 CMIP3 models (Meehl et al., 2007). A summary of all the models used is provided in the Supplemental Information (Tables S1-S3). Using bilinear interpolation, all CMIP3, CMIP5, and CMIP6 model variables were regridded to a common 1.0° lat./lon. grid before analysing. This spatial resolution is finer than the native grid resolution used in all but two of the CMIP6 models. Results using the two highest resolution CMIP6 models at their native resolution (not shown) where very similar to those regridded to the 1.0° resolution. Monthly climatologies were computed for all model variables using a base period of 1981-2010 for CMIP6, 1979-2005 for CMIP5, and 1971-2000 for CMIP3 using a single ensemble member from each model.

### 2.2 | Observational data

Monthly precipitation analyses utilized included the gaugebased Global Precipitation Climatology Center (GPCC v7) data gridded to 1.0° lat./lon. resolution (Becker et al., 2013); the gauge-based version TS 4.01 of monthly precipitation over global land areas from the Climatic Research Unit at the University of East Anglia (CRU; Harris and Jones, 2017) gridded to 0.5° lat./lon. resolution; version 1.1 of the satellite-based Precipitation Estimation from Remotely Sensed Information using Artificial Neural Networks (PERSIANN; Ashouri et al., 2015) gridded to a 0.25° lat./lon. spatial resolution; version 2.0 of the Climate Hazards Group Infrared Precipitation with Station data (CHIRPS; Funk et al., 2015) gridded to a 0.05° lat./lon. resolution and version 2.3 of the Global Precipitation Climatology Project (GPCP) merged gauge and satellite estimate product (Huffman et al., 2009) at 2.5° lat./lon. resolution. Monthly climatologies were generated for these precipitation datasets using a 1981-2010 base period, with the exception of PERSIANN, where a 1983-2010 base period was used owing to data availability.

Monthly SST analyses from the Extended Reconstructed SST v4 dataset (ERSST; Huang *et al.*, 2015) at 2.0° lat./lon. resolution and the 1.0° lat./lon. optimum interpolation of SST v2 (OIv2; Reynolds *et al.*, 2002) were employed. The horizontal components of the 850 hPa wind field from the ERA-Interim reanalysis product (Dee *et al.*, 2011) were utilized and regridded to a common 1.0° lat./lon. grid. Monthly climatologies for a 1981–2010 base period were computed for ERSST and OIv2, with a 1971–2000 monthly climatology also constructed for ERSST.

RMetS

# 2.3 | Methodological approach

Locations in the Greater Horn having a bimodal rainfall annual cycle were identified following the method detailed in the study by Lyon (2020) and are shown by the shaded area in the inset in Figure 1a. Observational and model rainfall data are projected onto this area in the analysis. Coupled model biases in SST are identified by subtracting the observed monthly SST climatology from the model climatology, using OIv2 (1981-2010) for CMIP6 and ERSST (1971-2000) for CMIP3 and CMIP5. Similarly, model biases in climatological rainfall and 850 hPa horizontal wind are computed by subtracting observed monthly climatological values from the model climatology, using GPCP for observed rainfall (Lyon and DeWitt (2012) found similar results to GPCP using other merged rainfall datasets for this region) and ERA-Interim for 'observed' wind. Statistically significant differences for all variables were determined using a two-tailed t-test at the 95% confidence level unless otherwise noted. For the 850 hPa wind, at least one component needed to be significant with both components shown on plots.

#### 3 | RESULTS

# 3.1 | MMM biases in the annual cycle of Greater Horn rainfall

The climatological annual cycle of rainfall for four observational datasets and the 21 CMIP6 models is shown in Figure 1a, with the difference between the MMM values and the mean of observed datasets shown in Figure 1b. In addition to obvious monthly amplitude biases, the MMM of the CMIP6 models displays the same major biases identified in CMIP3 and CMIP5, with the OND short rains being too wet relative to observations, the MAM long rains being too dry, and there is a 1-month lag in the peak of the long rains in CMIP6 relative to observations. In 19 of the 21 CMIP6 models (90%), OND rainfall exceeds that in MAM and 16 of the 21 models (76%) show climatological May rainfall greater than that in April. Figure 1c shows the annual cycle for the mean of the four observational datasets along with the MMM values for CMIP3, CMIP5, and CMIP6. The temporal correlation of the annual cycle between observations and the MMM is r = .70 for CMIP3, r = .54 for CMIP5, and r = .70 for CMIP6. The correlation of the MMM annual cycles is r = .96 between CMIP3 and CMIP5, r = .96between CMIP5 and CMIP6, and r = .99 between CMIP3 and CMIP6. The CMIP MMM annual cycles are thus in very close agreement with each other but much less so with observations. The MMM root-mean-square error

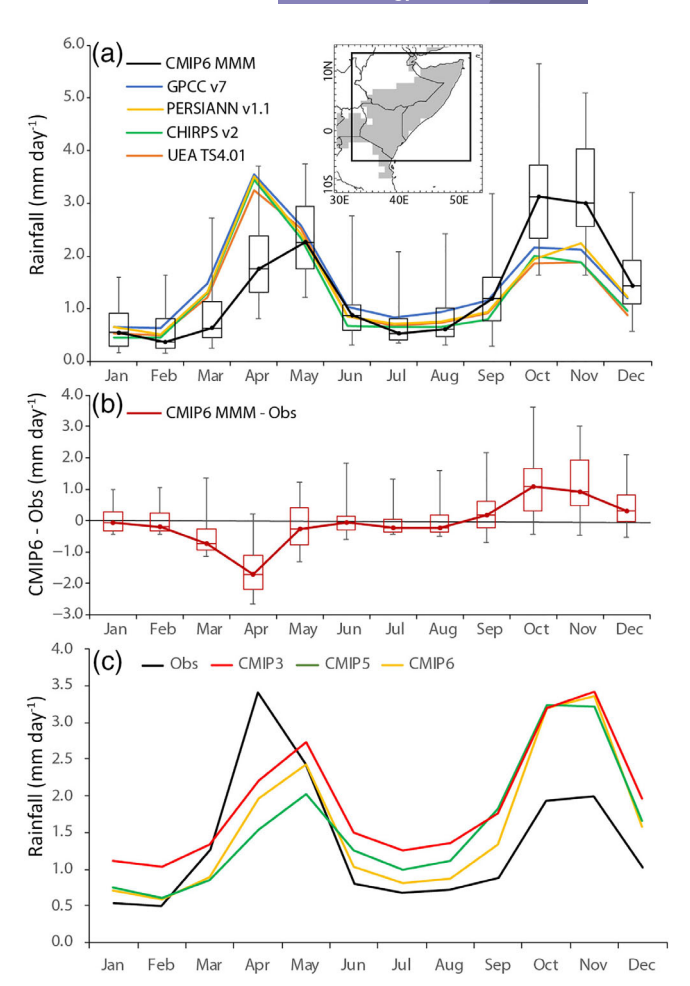


FIGURE 1 (a) Monthly climatological rainfall (mm day<sup>-1</sup>) for shaded study domain of the Greater Horn (inset) for four observational datasets and the CMIP6 multi-model mean (solid black line), with boxes showing the interquartile range and whiskers indicating overall model range. (b) Difference between the CMIP6 multi-model mean and mean of the observational datasets (mm day<sup>-1</sup>) shown as the solid red line with box and whiskers again showing model ranges. (c) Rainfall annual cycle (mm day<sup>-1</sup>) for the mean of the four observational datasets (black line) and the multi-model mean of 20 CMIP3 models (red line), 31 CMIP5 models (green line) and 21 CMIP6 models (gold line) [Colour figure can be viewed at wileyonlinelibrary.com]

(RMSE) in the monthly climatologies (in mm day<sup>-1</sup>) is 1.12 for CMIP3, 1.11 for CMIP5, and 0.97 for CMIP6. Thus, in the MMM, the CMIP6 models show some marginal improvement in simulating the annual cycle over CMIP3 and CMIP5 (although the CMIP5 models showed little improvement over CMIP3, as also found by Koutroulis *et al.*, 2016).

As seen in Figure 1b, the largest differences between the CMIP6 MMM annual cycle and observations occur in the months of March and April (MA) during the long rains and October and November (ON) during the short rains. These two periods were therefore examined in greater detail. Figure 2a,b shows the regional bias in the MMM climatological rainfall and 850 hPa vector wind for MA and ON, respectively. For MA (Figure 2a), the MMM of the CMIP6 models show a north-south oriented rainfall bias pattern, with generally too little (too much) rainfall north (south) of the equator. The associated 850 hPa wind bias pattern generally opposes the observed climatological flow (not shown) over the Greater Horn and western Indian Ocean, with an associated easterly wind bias north of the equator over the Indian Ocean. This is consistent with a delay in the

annual cycle, as was shown in earlier studies of the CMIP5 annual cycle bias for the Greater Horn (e.g., Yang et al., 2015; Lyon, 2020). Figure 2b shows that the MMM, positive rainfall bias over the Greater Horn for ON is part of a larger, zonally elongated region of enhanced rainfall centred roughly along the equator. The bias in the 850 hPa wind field acts to enhance the climatological flow (not shown) into the Greater Horn in ON, consistent with the wetter than observed conditions there. Similar biases were identified in the CMIP5 rainfall and wind fields (e.g., Lyon, 2020).

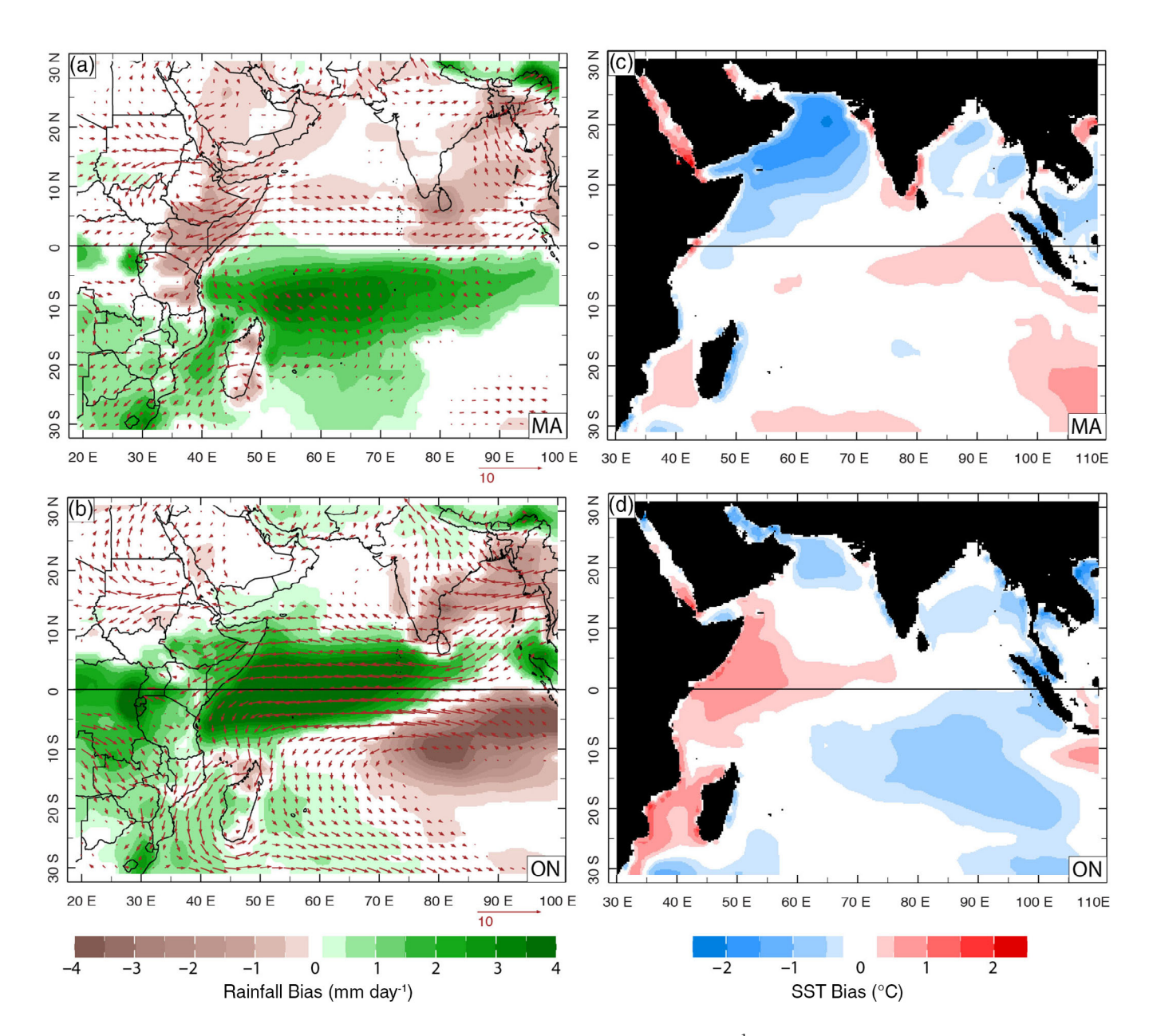


FIGURE 2 (a) CMIP6 multi-model mean climatological rainfall bias (shaded, mm day<sup>-1</sup>), along with bias in vector wind at 850 hPa (representative vector in lower-right, units are m s<sup>-1</sup>) for the months of March and April (MA). Only statistically significant (p < .05) biases are plotted (at least one component for wind). (b) As in (a) except for the months of October and November (ON). (c) Corresponding multi-model mean sea surface temperature (SST) bias for March and April ( $^{\circ}$ C). (d) As in (c) but for the months of October and November [Colour figure can be viewed at wileyonlinelibrary.com]

The CMIP6 MMM SST biases for MA and ON are shown in Figure 2c,d, respectively. Again, similar to CMIP5, the CMIP6 models exhibit a cold SST bias in the northern Indian Ocean during MA, with an east-west dipole SST bias pattern seen for ON (Figure 2d), reminiscent of the Indian Ocean Dipole mode (IOD; Saji et al., 1999) which Cai and Cowan (2013) show is too strong in CMIP5 relative to observations. These SST bias patterns are generally consistent with the rainfall bias patterns. As mentioned in the Introduction, Lyon (2020) linked the MMM SST bias pattern in CMIP5 models to biases in Greater Horn annual cycle based on model experiments with an AGCM. For the domain shown in Figure 2, the pattern correlation between the MMM SST bias pattern in CMIP6 with that in CMIP5 is  $r_{\rm pc} = .86$  for the MA season and  $r_{\rm pc}$  = .78 for ON. For the CMIP5 MMM, Lyon (2020) showed a close association between the annual cycle of the bias in Greater Horn rainfall and the IOD index computed from climatological SST. For CMIP6, the temporal correlation between the two is r = .64, which is statistically significant (p < .01). For the global domain (40°S-40°N), the pattern correlation of the MMM SST biases in CMIP6 and CMIP5 is  $r_{\rm pc} = .92$  for the MA season and  $r_{pc} = .93$  for ON.

# 3.2 | Examination of the best performing models

The MMM results presented in the previous subsection may mask the behaviour of the best performing models within the three CMIP phases. As such, the three best performing models were identified for CMIP3, CMIP5, and CMIP6 based on the combination of highest correlation and lowest RMSE when compared with the observed climatological annual cycle of Greater Horn rainfall. As a first step, Figure 3 shows the correlation versus the RMSE for each model analysed from CMIP3, CMIP5, and CMIP6 (median values for each model group are also plotted). Note that there is not a clear separation in model behaviour across the three CMIP classes. In fact, based on Kolmogorov-Smirnov tests applied separately to correlation and RMSE, when all models are considered within each CMIP group, there is not a statistically significant difference in CMIP6 model performance over CMIP5 or CMIP3. However, based on this analysis, the three best performing models in each CMIP group (data points in the upper-left of Figure 3) were selected for further analysis.

The mean annual cycles for the three best performing models within each CMIP group are plotted in Figure 4a, along with the monthly mean values from the observational datasets. The correlations between the modelled and observed annual cycles for the three best performing

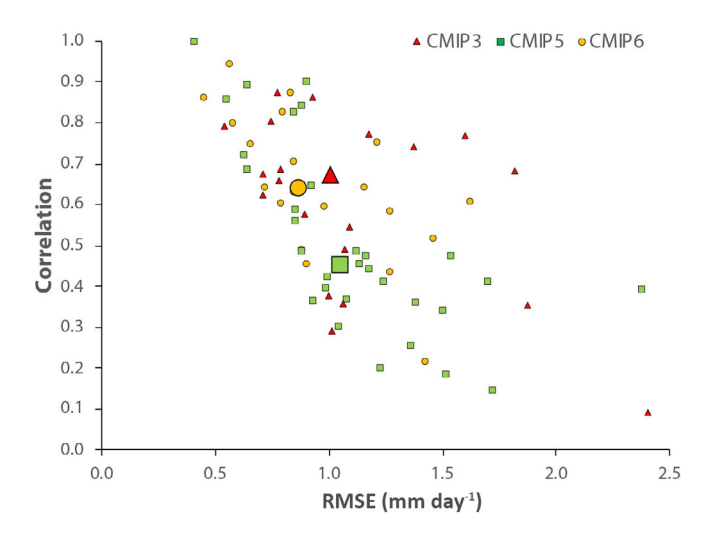


**FIGURE 3** Correlation versus root-mean-square error (RMSE) (mm day<sup>-1</sup>) of the modelled climatological annual cycle of Greater Horn rainfall for all models used in the study from CMIP3 (red symbols), CMIP5 (green) and CMIP6 (gold). The larger symbols indicate the median values for each CMIP group [Colour figure can be viewed at wileyonlinelibrary.com]

models are r = .84 for CMIP3, r = .96 for CMIP5, and r = .92 for CMIP6. The corresponding RMSE values (in mm day<sup>-1</sup>) are 0.53 for CMIP3, 0.49 for CMIP5, and 0.35 for CMIP6. As mentioned in Section 3.1, in the MMM, the CMIP models tend to generate too much rainfall in OND relative to MAM and there is typically a 1-month delay in the peak of the long rains relative to observations. For the three best performing models, both of these model biases were still observed for CMIP3, while only the first (OND > MAM rainfall) bias was observed for the three best performing CMIP5 and CMIP6 models. By these measures, the three best CMIP6 models show incremental improvements in performance relative to CMIP3, with mixed results in terms of improvements over CMIP5. It is interesting to note that the best performing models are not necessarily those with the highest spatial resolution. Figure 4b shows the mean annual cycles for the three highest resolution models within each CMIP group. The correlations with the observed annual cycle are r = .75 for CMIP3, r = .45 for CMIP5, and r = .79 for CMIP6. The associated RMSE values (in mm day<sup>-1</sup>) are 0.96 for CMIP3, 1.00 for CMIP5, and 0.59 for CMIP6. Thus, while the three CMIP6 models with the highest spatial resolution outperform their CMIP5 and CMIP3 counterparts, they are not the best performing models overall. This result is found to be more general, as shown in Supplemental Figure S1, where no statistically significant relationship is found between model performance (correlation, RMSE) and model spatial resolution when the Greater

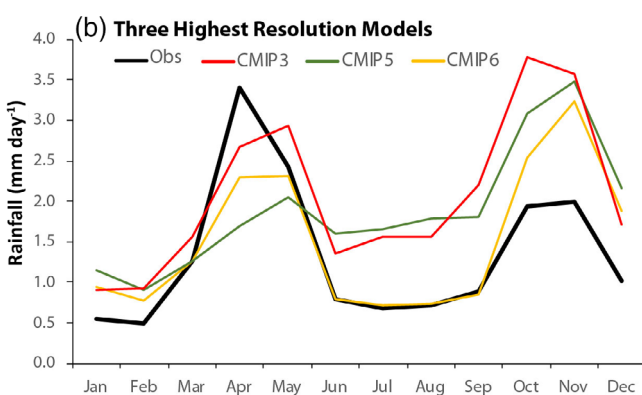


FIGURE 4 (a) Climatological annual cycles of Greater Horn rainfall (mm day<sup>-1</sup>) for the mean of the four observational datasets (black line) and the mean of the three best performing models from CMIP3 (red line), CMIP5 (green line) and CMIP6 (gold line). (b) As in (a), but for the three models with the highest spatial resolution from each CMIP group [Colour figure can be viewed at wileyonlinelibrary.com]

Horn climatological annual cycle is examined for each model within the three CMIP groups.

Since model resolution is not a reliable predictor of model performance in simulating the climatological annual cycle of Greater Horn rainfall, previous results suggest that improved model performance may instead be tied to a more realistic simulation of the SST annual cycle. As an initial step towards investigating this possibility, differences in climatological SST and 850 hPa vector wind were computed between the three best performing CMIP6 models and the mean of the 18 remaining CMIP6 models for the spatial domain used in Figure 2. These differences were computed for the MA and ON seasons when the CMIP6 MMM biases in Greater Horn rainfall are largest (c.f. Figure 1). The results are shown in Figure 5. For the MA season (Figure 5a), the difference in SST features a warmer (cooler) northern (southern) Indian Ocean in the three best performing models, generally opposing the MMM biases shown in Figure 2c. The 850 hPa wind differences show an enhanced southwesterly flow across the eastern Greater Horn and western Indian Ocean, generally opposing the MMM wind bias pattern seen in

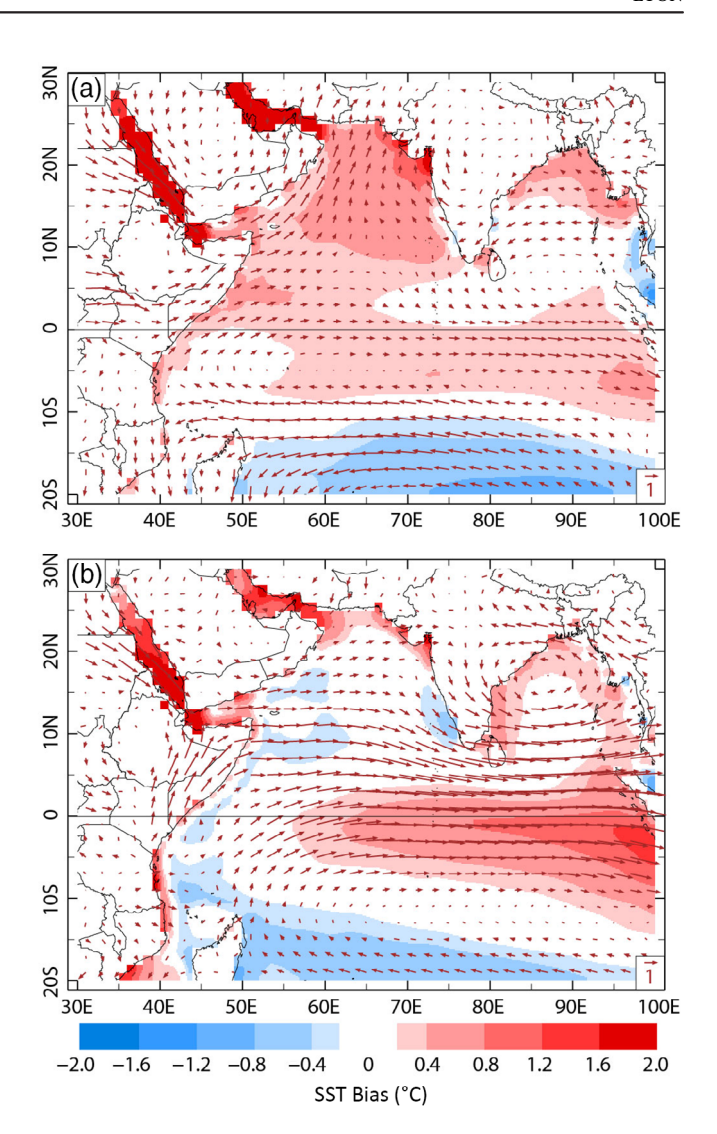


FIGURE 5 (a) Difference in climatological sea surface temperature (SST) (shading) and 850 hPa wind (representative vector at lower-right in m s<sup>-1</sup>) between the three best performing CMIP6 models and the 18 remaining models for the months of March and April. (b) As in (a), but for the months of October and November [Colour figure can be viewed at wileyonlinelibrary.com]

Figure 2a. For the ON season, SSTs in the equatorial eastern (western) Indian Ocean are warmer (cooler) in the three best performing models, generally opposite of the MMM SST bias pattern seen in Figure 2d. The 850 hPA wind differences for ON feature westerlies across the equatorial Indian Ocean and southwesterlies across the eastern Greater Horn, both generally opposite of the MMM biases (Figure 2b). The pattern correlation in Indian Ocean SST for the three best CMIP6 models and the remaining CMIP6 models is  $r_{\rm pc}=.57$  for MA and  $r_{\rm pc}=.70$  for ON. The corresponding pattern correlations for the three highest resolution models and the remaining models (excluding the three best performing) are  $r_{\rm pc}=.82$  for MA and  $r_{\rm pc}=.82$  for ON. While preliminary, these findings support the earlier conclusion based on the

analysis of CMIP5 models, that properly simulating the annual cycle of SSTs is key to capturing the observed annual cycle of Greater Horn climatological rainfall.

# 4 | SUMMARY AND CONCLUSIONS

A fundamental problem, common to most CMIP3 and CMIP5 coupled climate models, was their inability to properly capture the bimodal rainfall annual cycle across the Greater Horn of Africa. Here, the climatological rainfall annual cycle was examined in 21 CMIP6 models, with the MMM results showing that the biases seen in the previous two CMIP model phases persist in the latest generation of coupled models, with the short rains (long rains) of OND (MAM) being much too wet (too dry) relative to observational datasets. In the MMM, there also continues to be a distinct, 1-month lag in the peak of the long rains relative to observations in CMIP6 (rainfall peaks in May rather than in April as observed).

Lyon (2020) showed that CMIP5 climatological SST biases were directly linked to biases in the annual cycle of rainfall in the Greater Horn. Over the global domain (40°S-40°N), the pattern correlation between the MMM SST bias patterns in the CMIP6 and CMIP5 historical runs is  $r_{pc} = .92$  for MA and  $r_{pc} = .93$  for ON, the two periods showing the largest model biases in Greater Horn rainfall. Over the Indian Ocean, the pattern correlation between the MMM SST bias patterns in CMIP6 and CMIP5 is  $r_{pc} = .86$  for MA and  $r_{pc} = .78$  for ON. As with CMIP5, CMIP6 models again have historical SST biases that map onto the positive phase of the IOD, a mode of variability known to influence Greater Horn rainfall (Black et al., 2003), with McKenna et al. (2020) finding generally modest changes in the historical behaviour of the IOD in CMIP6 compared with CMIP5. The temporal correlation between the monthly biases in the climatological annual cycles of Greater Horn rainfall bias and MMM IOD in the CMIP6 MMM is r = .64, which is statistically significant at p < .01.

To examine whether the MMM results obscure incremental improvements in the top performing CMIP6 models, the three best performing models (based on RMSE and correlation with observations) within each CMIP group were examined in greater detail. The mean annual cycle for the three best performing CMIP6 models exhibited a lower RMSE than the CMIP3 or CMIP5 counterparts and a correlation with observations that was higher than CMIP3 but slightly lower than that for the top CMIP5 models. There was not a 1-month delay in the peak of the MAM long rains for the top CMIP6 models, but OND rainfall remained slightly more than MAM, contrary to observations. Overall, for the best performing models, CMIP6 shows improvement over CMIP3, with mixed results in terms of improvements over CMIP5. Interestingly, the top three performing CMIP6 models were not necessarily those with the highest spatial resolution (this was also a general finding when all models within CMIP3, CMIP5, and CMIP6 were evaluated). Rather, the enhanced performance of the CMIP6 models was found to be related to reduced climatological biases in Indian Ocean SST and 850 hPa wind. This result suggests that improved simulation of the climatological annual cycle in Greater Horn rainfall depends fundamentally on the model's ability to properly capture the climatological annual cycle of SSTs.

#### **ACKNOWLEDGEMENTS**

The World Climate Research Programme is acknowledged, which, through its Working Group on Coupled Modelling, coordinated and promoted CMIP6. The author thanks the climate modelling groups for producing and making available their model output, the Earth System Grid Federation (ESGF) for archiving the data and providing access, and the multiple funding agencies who support CMIP6 and ESGF. The author also thanks Haibo Liu of the Lamont Doherty Earth Observatory for his substantial assistance in obtaining and analysing the CMIP3, CMIP5 and CMIP6 coupled model data. Helpful comments by the reviewers served to improve the original version of the manuscript. This work was supported by a grant from the National Science Foundation, Award AGS 1650037, which is gratefully acknowledged.

# CONFLICT OF INTEREST

The author has no conflict of interest to declare.

# ORCID

*Bradfield Lyon* https://orcid.org/0000-0002-1364-7845

# REFERENCES

Anyah, R.O. and Qiu, W. (2011) Characteristic 20th and 21st century precipitation and temperature patterns and changes over the Greater Horn of Africa. International Journal of Climatology, 31, 2081-2097.

Ashouri, H., Hsu, K., Sorooshian, S., Braithwaite, D.K., Knapp, K. R., Cecil, L.D., Nelson, B.R. and Prat, O.P. (2015) PERSIANN-CDR: daily precipitation climate data record from multisatellite observations for hydrological and climate studies. Bulletin of the American Meteorological Society, 96, 69-83.

Becker, A., Finger, P., Meyer-Christoffer, A., Rudolf, B., Schamm, K., Schneider, U. and Ziese, M. (2013) A description of the global land-surface precipitation data products of the global precipitation climatology centre with sample applications including centennial (trend) analysis from 1901-present. Earth System Science Data, 5, 71-99. https://doi.org/10.5194/ essd-5-71-2013.

Black, E., Slingo, J. and Sperber, K.R. (2003) An observational study of the relationship between excessively strong short rains in

- coastal East Africa and Indian Ocean SST. Monthly Weather Review, 131, 74-94.
- Cai, W. and Cowan, T. (2013) Why is the amplitude of the Indian Ocean dipole overly large in CMIP3 and CMIP5 climate models? *Geophysical Research Letters*, 40, 1200–1205.
- Conway, D., Dalin, C., Landman, W.A. and Osborn, T.J. (2017) Hydropower plans in eastern and southern Africa increase risk of concurrent climate-related electricity supply disruption. *Nature Energy*, 2, 946–953.
- Dee, D.P., Uppala, S.M., Simmons, A.J., Berrisford, P., Poli, P., Kobayashi, S., Andrae, U., Balmaseda, M.A., Balsamo, G., Bauer, P., Bechtold, P., Beljaars, A.C.M., van de Berg, L., Bidlot, J., Bormann, N., Delsol, C., Dragani, R., Fuentes, M., Geer, A.J., Haimberger, L., Healy, S.B., Hersbach, H., Hólm, E. V., Isaksen, L., Kållberg, P., Köhler, M., Matricardi, M., McNally, A.P., Monge-Sanz, B.M., Morcrette, J.J., Park, B.K., Peubey, C., de Rosnay, P., Tavolato, C., Thépaut, J.N. and Vitart, F. (2011) The ERA-interim reanalysis: configuration and performance of the data assimilation system. *Quarterly Journal of the Royal Meteorological Society*, 137, 553–597.
- Dunning, C.M., Allan, R.P. and Black, E. (2017) Identification of deficiencies in seasonal rainfall simulated by CMIP5 climate models. *Environmental Research Letters*, 12, 114001. https://doi.org/10.1088/1748-9326/aa869e.
- Eyring, V., Bony, S., Meehl, G.A., Senior, C.A., Stevens, B., Stouffer, R.J. and Taylor, K.E. (2016) Overview of the coupled model intercomparison project phase 6 (CMIP6) experimental design and organization. *Geoscientific Model Development*, 9, 1937–1958.
- Funk, C.P., Peterson, P., Landsfeld, M., Pedreros, D., Verdin, J., Shukla, S., Husak, G., Rowland, J., Harrison, L., Hoell, A. and Michaelsen, J. (2015) The climate hazards infrared precipitation with stations—a new environmental record for monitoring extremes. *Scientific Data*, 2, 150066. https://doi.org/10.1038/ sdata.2015.66.
- Hamlet, A., Jean, K., Perea, W., Yactayo, S., Biey, J., Van Kerkhove, M., Ferguson, N. and Garske, T. (2018) The seasonal influence of climate and environment on yellow fever transmission across Africa. *PLoS Neglected Tropical Diseases*, 12, e0006284.
- Hansen, J.W. (2005) Integrating seasonal climate prediction and agricultural models for insights into agricultural practice. *Philo-sophical Transactions of the Royal Society B: Biological Sciences*, 360, 2037–2047.
- Harris, I.C. and Jones, P.D. (2017) CRU TS4.01: climatic research unit (CRU) time-series (TS) version 4.01 of high-resolution gridded data of month-by-month variation in climate (Jan. 1901–Dec. 2016). Centre for Environmental Data Analysis, Available at: http://catalogue.ceda.ac.uk/uuid/ 58a8802721c94c66ae45c3baa4d814d0 [Accessed 23rd November 2020].
- Huang, B., Banzon, V.F., Freeman, E., Lawrimore, J., Liu, W., Peterson, T.C., Smith, T.M., Thorne, P.W., Woodruff, S.D. and Zhang, H.M. (2015) Extended Reconstructed Sea surface temperature version 4 (ERSST.v4). Part I: upgrades and intercomparisons. *Journal of Climate*, 28, 911–930.
- Huffman, G.J., Adler, R.F., Bolvin, D.T. and Gu, G. (2009) Improving the global precipitation record: GPCP version 2.1.

- Geophysical Research Letters, 36, L17808. https://doi.org/10.1029/2009GL040000.
- Koutroulis, A.G., Grillakis, M.G., Tsanis, I.K. and Papadimitriou, L. (2016) Evaluation of precipitation and temperature simulation performance of the CMIP3 and CMIP5 historical experiments. *Climate Dynamics*, 47, 1881–1898.
- Lyon, B. (2020) Biases in CMIP5 sea surface temperature and the annual cycle of east African rainfall. *Journal of Climate*, 33, 8209–8223.
- Lyon, B. and DeWitt, D.G. (2012) A recent and abrupt decline in the East African long rains. *Geophysical Research Letters*, 39, L02702. https://doi.org/10.1029/2011GL050337.
- Lyon, B. and Vigaud, N. (2017) Unraveling East Africa's climate paradox. In: Wang, S.-Y.S., Yoon, J.-H., Funk, C.C. and Gillies, R.R. (Eds.) *Climate Extremes: Patterns and Mechanisms*. Hoboken, NJ: Wiley, pp. 265–281.
- McKenna, S., Santoso, A., Gupta, A.S., Taschetto, A.S. and Cai, W. (2020) Indian Ocean dipole in CMIP5 and CMIP6: characteristics, biases, and links to ENSO. *Scientific Reports*, 10, 1–13.
- Meehl, G.A., Covey, C., Delworth, T., Latif, M., McAvaney, B., Mitchell, J.F., Stouffer, R.J. and Taylor, K.E. (2007) The WCRP CMIP3 multimodel dataset: a new era in climate change research. Bulletin of the American Meteorological Society, 88, 1383–1394.
- Otieno, V.O. and Anyah, R.O. (2013) CMIP5 simulated climate conditions of the Greater Horn of Africa (GHA). Part I: contemporary climate. *Climate Dynamics*, 41, 2081–2097.
- Reynolds, R.W., Rayner, N., Smith, T., Stokes, D. and Wang, W. (2002) An improved in situ and satellite SST analysis for climate. *Journal of Climate*, 15, 1609–1625.
- Saji, N.H., Goswami, B.N., Vinayachandran, P.N. and Yamagata, T. (1999) A dipole mode in the tropical Indian Ocean. *Nature*, 401, 360–363.
- Taylor, K.E., Stouffer, R.J. and Meehl, G.A. (2012) An overview of CMIP5 and the experiment design. Bulletin of the American Meteorological Society, 93, 485–498.
- Thomson, M.C., Ukawuba, I., Hershey, C.L., Bennett, A., Ceccato, P., Lyon, B. and Dinku, T. (2017) Using rainfall and temperature data in the evaluation of national malaria control programs in Africa. *The American Journal of Tropical Medicine and Hygiene*, 97, 32–45.
- Yang, W., Seager, R., Cane, M.A. and Lyon, B. (2015) The rainfall annual cycle bias over East Africa in CMIP5 coupled climate models. *Journal of Climate*, 28, 9789–9802.

# SUPPORTING INFORMATION

Additional supporting information may be found in the online version of the article at the publisher's website.

**How to cite this article:** Lyon, B. (2021). Biases in sea surface temperature and the annual cycle of Greater Horn of Africa rainfall in CMIP6. *International Journal of Climatology*, 1–8. <a href="https://doi.org/10.1002/joc.7456">https://doi.org/10.1002/joc.7456</a>